Penerbit Akademia Baru

Journal of Advanced Research Design

Journal homepage:
https://akademiabaru.com/submit/index.php/ard
ISSN: 2289-7984

Design and Control of Integrated Distribution Static Synchronous Compensator with Grid-Connected Solar Photovoltaic System using FFT

Nur Fatini Ahmad Sobri[1], Nor Hanisah Baharudin[1,2,*], Tunku Muhammad Nizar Tunku Mansur[1,2], Rosnazri Ali[1,2], Aini Syahida Mohd Shaizad[1], Mohd Syahril Noor Shah[1,2], Muhd Hafizi Idris[1,2]

[1] Department of Electrical Engineering, Faculty of Electrical Engineering & Technology, University of Malaysia Perlis, 02600 Arau, Perlis, Malaysia
[2] Centre of Excellence for Renewable Energy (CERE), Faculty of Electrical Engineering & Technology, Universiti Malaysia Perlis, Pauh Putra Campus, 02600 Arau, Perlis, Malaysia

ARTICLE INFO

Article history:
Received 2 February 2025
Received in revised form 1 September 2025
Accepted 23 September 2025
Available online 1 October 2025

Keywords:
DSTATCOM, FFT, Power quality, Harmonic

ABSTRACT

This paper presents a Fast Fourier Transform (FFT) based Voltage Reference Configuration (VRC) control algorithm for the three phase Distribution Static Compensator (DSTATCOM) into grid-connected solar photovoltaic system for power quality improvement under nonlinear load and unbalanced load in distribution system It aims to address power quality issues characterized by voltage, current, or frequency deviations, which can lead to equipment failures. Conventional power grids typically deliver clean sinusoidal waveforms for reliable operation. However, the introduction of nonlinear loads introduces harmonic distortions, which can lead to problems such as transformer overheating and grid malfunctions. The proposed approach employs FFT to isolate harmonic components from the load current. These components are then utilized by a hysteresis current controller to regulate the Voltage Source Inverter (VSI). The study extensively models and simulates the system's performance under various conditions, including nonlinear and unbalanced loads, fluctuating solar irradiance levels, and dual-mode operation of the Grid-Connected Solar System based DSTATCOM (GCPV based DSTATCOM). Simulink is used in the MATLAB environment to carry out these simulations. The findings show that the suggested control method successfully complies with IEEE-519 by reducing harmonic distortion and keeping the Total Harmonic Distortion (THD) value below the permitted 5% limit. This achievement signifies a significant advancement in ensuring robust power quality in grid-connected solar photovoltaic systems.

1. Introduction

Power quality refers to any deviation in voltage, current, or frequency that leads to the failure or malfunction of customers' equipment [1][2]. The power supply provided by the utility grid is clean and sinusoidal waveforms that do not contain sags or spikes, which allows the customers' equipment to operate reliably [3]. The consumer load can be divided into two types which are linear loads and

* *Corresponding author.*
E-mail address: norhanisah@unimap.edu.my

https://doi.org/10.37934/ard.143.1.248260

nonlinear loads. The main concern is nonlinear, consisting of a harmonic component in the load current, and can cause harmonic distortions in the source current in the grid utility system [4] . The increase of usage of nonlinear load leads to harmonic distortions such as heating of transformer, natural conductor overloading, and malfunction of grid utility and consumer equipment [5]–[7]. Another challenge in distribution networks arises from the provision of unbalanced load currents, often attributed to traction drives and switch-mode power supplies [8].

The incorporation of the solar PV system into the distribution grid has led to power quality challenges, notably harmonic distortions [9]. The impacts of harmonics within power system networks can have significant and lasting consequences. Previous studies have highlighted concerns regarding power inverters interfacing with PV arrays in power grids, as they can generate harmonic currents. Consequently, this may elevate both the total harmonic distortion of voltage and current at the point of standard coupling (PCC) [10]. The frequency domain has been used for measuring the harmonic current in the nonlinear load [11], [12].

The proposed solution seeks to harness the DSTATCOM's capabilities to mitigate voltage fluctuations, harmonics, and load imbalances. This necessitates an intricate analysis of system components and control strategies to effectively enhance power quality, ensuring the seamless integration of solar-generated power while maintaining grid stability [13]. When combined with a frequency domain-based Voltage Reference Configuration (VRC) control algorithm, the proposed three-phase, three-wire Grid-Connected Solar Photovoltaic (GCPV) based DSTATCOM can mitigate distribution system power quality problems.

The frequency domain based VRC control algorithm technique uses Fourier analysis to extract the harmonic component from the distorted voltage or current signal [14]. It is already applied in single-phase and three single-phase active power filters, and it has been proved that this controller is a simpler, robust control scheme and less computational time for extracting reference current signals [15]. All the simulations were simulated using MATLAB/SIMULINK.

After obtaining the simulation analysis results using the MATLAB Simulink environment, the proposed prototype is implemented into a real-time application using C2000™ Real-Time Control Microcontrollers (MCUs). Embedded Coder is harnessed to tailor the code derived from the MATLAB/Simulink algorithms. This process involves configuring software interfaces, fine-tuning execution performance, and minimizing memory utilization for optimized control [16].

2. Methodology

2.1 DSTATCOM System Configuration

2.1.1 DC bus voltage

The value of the PCC voltage has a direct impact on the DC bus voltage (V_{dc}) to achieve successful pulse width modulation (PWM) control of the Voltage Source Converter (V_{SC}) in a DSTATCOM. Specifically, the DC bus voltage needs to be greater than the amplitude of the AC mains voltage. Eq. (1) defines the DC bus voltage for a three-phase Voltage Source Converter (V_{SC}).

$$V_{dc} = \frac{2\sqrt{2}\ V_{LL}}{\sqrt{3}(m)} \tag{1}$$

Where m is the modulation index and is considered as 1, while V is the AC line output voltage of DSTATCOM which is 415V. The value of V_{dc} is obtained as 677V using Eq. (1) and was picked as 700V.

2.1.2 DC bus capacitor

The instantaneous energy available to DSTATCOM and the second harmonic or ripple voltage in the DC bus voltage determine the value of the DC bus capacitor. The DC bus capacitor for a three-phase VSC is defined by Eq. (2).

$$C_{dc} = \frac{I_o}{2\omega \Delta V dc_{rip}} \tag{2}$$

where ω is the angular frequency, $Vdcrip$ is the ripple in the capacitor voltage, and Io is the capacitor current. Using Eq. (2), the value obtained for Cdc is 12279μF, taking into account that Io is 138.88A, ω is 100π, and $Vdcrip$ is 18V. Hence, the chosen capacitor value is 13000 μF.

2.2.3 AC Inductors

The switching frequency, f_s, and ripple current, I_{crpp}, determine the value of the AC inductance. The current ripple created will be eliminated by an AC inductor. In terms of AC inductor value, L_f is defined by Equation (3).

$$L_f = \frac{mV_{dc}}{4 \times a \times f_s \times I_{crpp}} \tag{3}$$

Where *m* is the modulation index and is considered as 1, switching frequency, f_s is 1.8kHz, DC bus voltage, V_{dc} is 700V, over load factor, *a* is equal to 1.2 and I_{crpp} is 20.83A. Using Eq. (3), the value obtained for AC inductor, L_f is 4mH [17]

2.2 Design on frequency domain based VRC Control Algorithm

Figure 1 illustrates the envisaged control architecture of the system. A frequency domain-based Voltage Reference Configuration (VRC) control algorithm is used to implement the method for separating harmonic elements from load currents. This method, which uses fewer parameters, activates the Voltage Source Inverter (VSI)'s insulated gate bipolar transistors (IGBTs) to effectively remove harmonics [17]. Three primary sections comprise the complex control structure:

(a) Unit Template Calculation (In-phase and Quadrature-phase)
(b) Evaluation of Harmonic Components of the Load
(c) Calculating Reference Currents and VSI Switching.

Each of these elements is explained in more detail below:

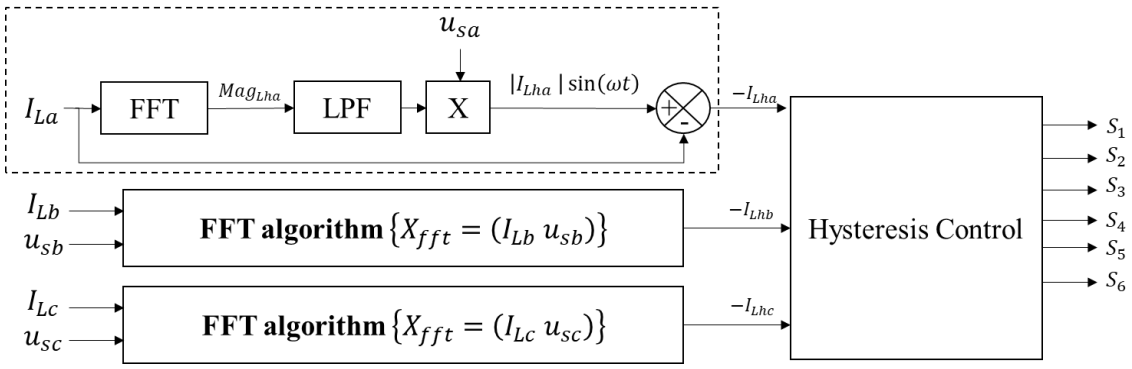

Fig .1. Frequency domain based VRC Control Algorithm

The line voltage (V_{sa},V_{sb},V_{sc}) is sensed at PCC. The in-phase component of the line voltage Eq. (4) is calculated by multiplying the constant value, in Eq. (5) to produce a sinusoidal unity wave in Equation Eq. (6).

$$V_{sa} = \sqrt{2}\ x\ 240\ \ sin(\omega t) \tag{4}$$

$$c = \frac{1}{\sqrt{2}\ x\ 240} \tag{5}$$

$$fa = \frac{1}{\sqrt{2}\ x\ 240}\ x\ \sqrt{2}\ x\ 240\ \ sin(\omega t) \tag{6}$$

The same goes for V_{sb} and V_{sc} in Eq. (7) to Eq. (8).

$$fb = V_{sb}\ x\ c \tag{7}$$

$$fc = V_{sc}\ x\ c \tag{8}$$

The FFT algorithm is employed to determine the approximate fundamental components of harmonics within a load. Assuming a symmetrical load current, Eq. (9) depicts the harmonic component of the load current through the application of the FFT rule for I_{La}. Thus, the 5th and 7th harmonics make up the load current. Even harmonics were produced and the odd harmonics were eliminated by the FFT block.

$$I_L(t) = \sum_{n=1}^{\infty} \frac{2I_A}{n\pi} sin\left(\frac{n\pi}{2}\right) cos(2\pi f t) \tag{9}$$

Next, the magnitude of the harmonic component was filtered using a low-pass Butterworth filter to achieve an improved initial response. A low pass filter can extract. The same goes for I_{Lc} and I_{Lc} in Eq. (10) to Eq. (11)

$$I_L(t) = \sum_{n=1}^{\infty} \frac{2I_B}{n\pi} sin\left(\frac{n\pi}{2}\right) cos(2\pi f t) \tag{10}$$

$$I_L(t) = \sum_{n=1}^{\infty} \frac{2I_C}{n\pi} sin\left(\frac{n\pi}{2}\right) cos(2\pi ft) \tag{11}$$

As shown in Figure 2, the hysteresis gap determines the estimation of the reference signal generation. By comparing it to the compensator current coming from the VSI output, the bang-bang theory is used to determine the upper and lower limits of the reference signal [18].

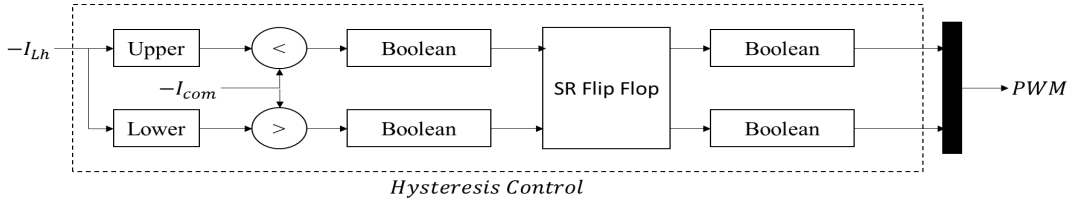

Fig .2. Hysteresis Current Control

2.3 Hardware-in-the-loop (HIL)

Hardware-in-loop (HIL) simulation requires the availability of analogue signal inputs from voltage and current sensors in order to generate a Pulse Width Modulation (PWM) signal. Still, these analog signals cannot be processed by MATLAB Simulink's control algorithm block until they are converted to digital form via an analog-to-digital converter (ADC). The digital signals that are produced are then utilised to produce a pulse signal, which triggers the inverter's gate switch and produces the PWM signal [16].

The voltage and current sensors must be calibrated in order to guarantee the correctness of the Hardware-in-loop (HIL) prototype output. MATLAB Simulink is used in these calibration phases to modify the gain and offset for the sensors. The DC supply can be used to alter the offset for zero voltage and current and the gain for voltage and current. To get reliable measurements under various operating conditions, perform this method numerous times.

The calibration makes sure that there is very little mistake and maximum precision in the conversion of the analogue signals from the sensors to their corresponding digital values. The calibrated sensors supply precise input to the MATLAB Simulink control algorithm block, which creates pulse signals to activate the inverter's gate switch and produce the Pulse Width Modulation (PWM) signal [19]. This PWM signal is then fed back to the HIL system to complete the feedback loop and verify the performance of the control algorithm in real-time.

2.4 Circuit Design
2.4.1 GCPV based DSTATCOM

Figure 3 displays the proposed GCPV-based DSTATCOM Simulink Model with frequency domain-based VRC Control Algorithm. The control algorithms that are used to generate the gating pulse and estimate the reference current have a significant impact on DSTATCOM's dynamic performance [20]. The reference source current includes an essential fundamental frequency component that is obtained from the load current and is necessary to determine when to switch on the DSTATCOM. These methods are used to extract this component. Using the source voltage, dc bus voltage, and load current as estimates, DSTATCOM will generate the desired current using a control algorithm. In order to produce the desired current into the DSTATCOM phase, VSI received the pulse gating signal generated by the hysteresis current control. By deducting the load current from the reference supply

current and obtaining the compensating currents for the DSTATCOM phase, the DSTATCOM satisfies the load's harmonic requirement [14].

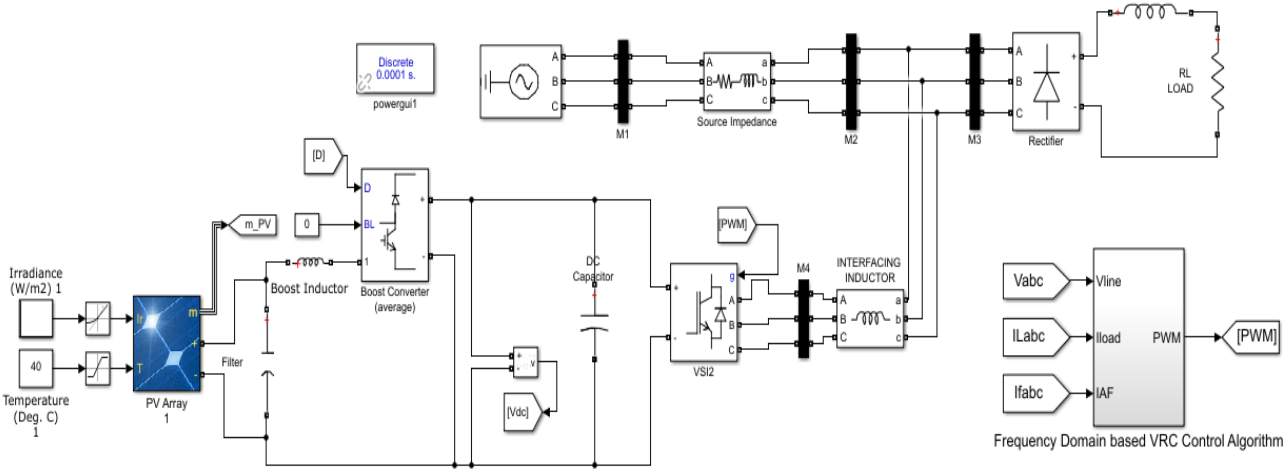

Fig .3. The PV-DSTATCOM Simulink Model with frequency domain based VRC Control Algorithm

2.4.2 Hardware-in-loop (HIL) Prototype

The three-phase DSTATCOM prototype was created using the TPS2014 Bench Digital Oscilloscope, which recorded waveforms and THD test results. Additionally, the DC supply, RL load (50 Ω and 150mH), inverter, three-phase rectifier, DC link capacitor, and C2000TM Real-Time Control Microcontrollers (MCUs) were utilised in the development of the prototype. Figure 4 illustrates this process.

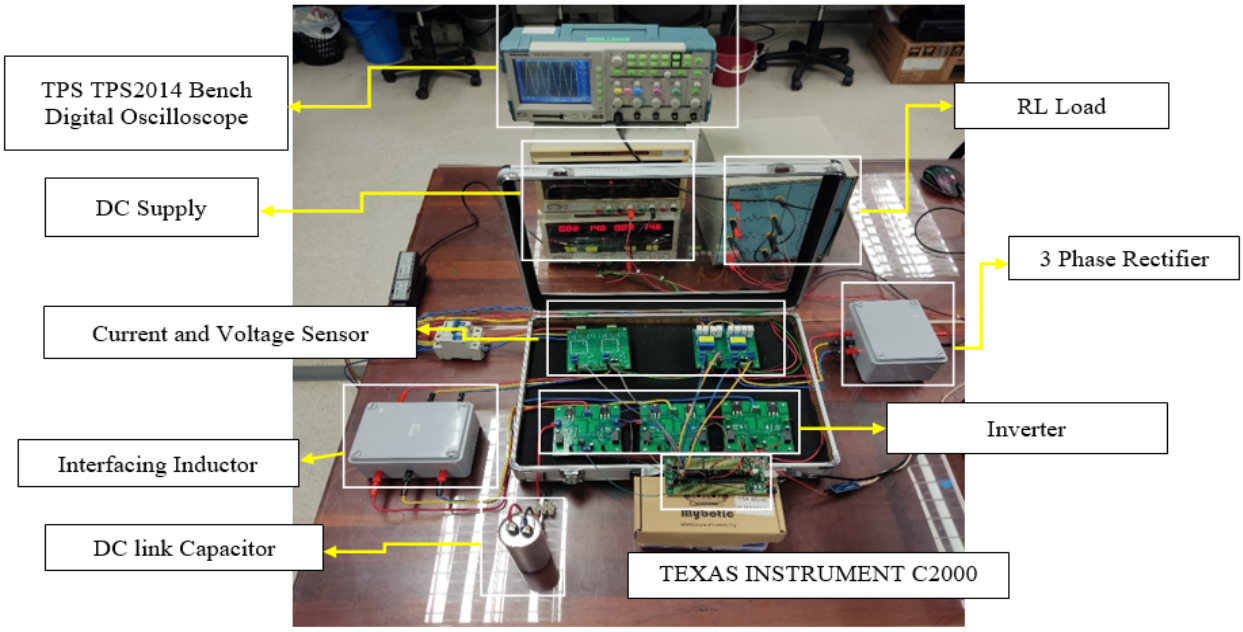

Fig .4. DSTATCOM HIL prototype

3. Results

3.1 GCPV based DSTATCOM Performance under Nonlinear Load

Figure 5 shows the scenario without the DSTATCOM in the analysis of the system's steady-state response under nonlinear load conditions. In this case, the source current (I_{Sabc}) THD value was measured at 22.48%.

Upon integrating the DSTATCOM after the load connection, both the load current and grid current exhibited a THD value of 22.48%, as depicted in Figure 6(a). On the other hand, Figure 6(b) shows that a useful amount of the harmonics were effectively routed to the grid, which led to a notable decrease in the grid current's THD value to just 1.42%. The source current waveform in Figure 5(a), which is sinusoidal and distortion-free, demonstrates how comfortably this reduction complied with the IEEE-519 standard's allowable limit of 5%.

This outcome underscores the commendable performance of the Voltage Source Inverter (VSI) within the DSTATCOM. It adeptly supplied the necessary harmonics at the Point of Common Coupling (PCC) to cater to the demands of the nonlinear load. As a result, the grid current exhibited a smooth, distortion-free waveform, ensuring the stability and high quality of the power supply.

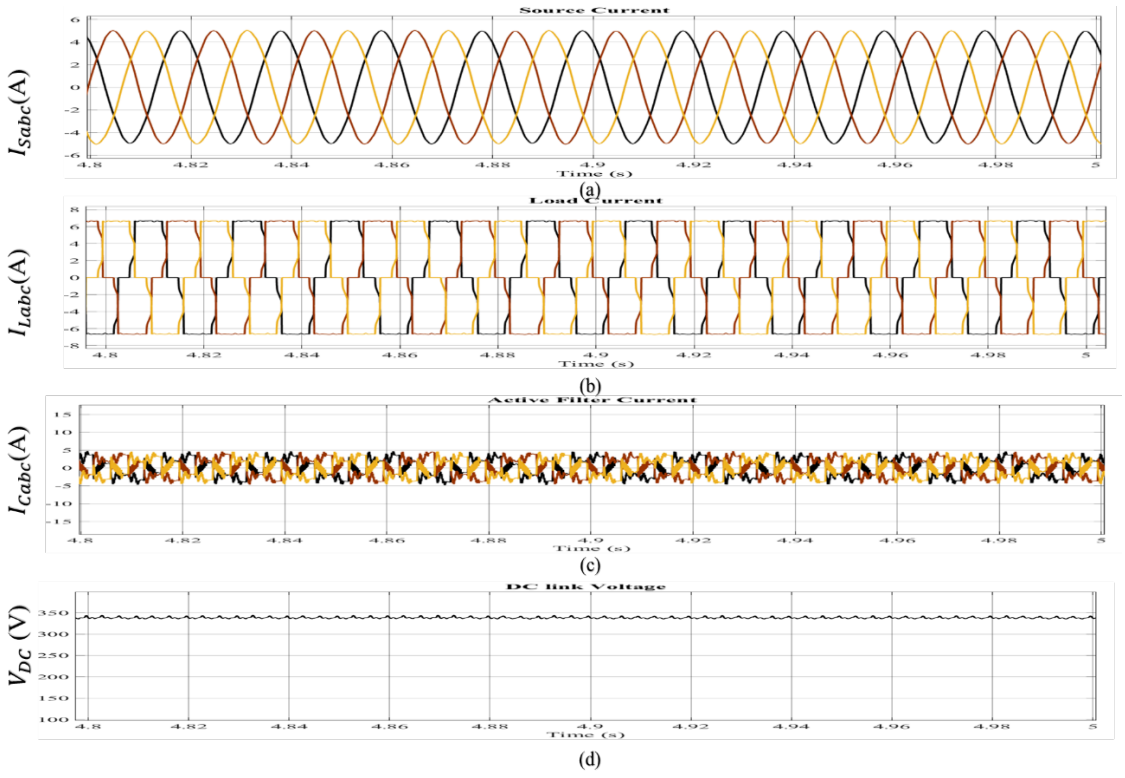

Fig .5. Steady state condition of the GCPV based DSTATCOM. (a) Source current (I_{sa} ,I_{sb} & I_{sc}) (b) Load current (I_{La} ,I_{Lb} & I_{Lc}) (c) Active Filter current (I_{ca} ,I_{cb} & I_{cc}) and (d) DC link voltage (V_{DC})

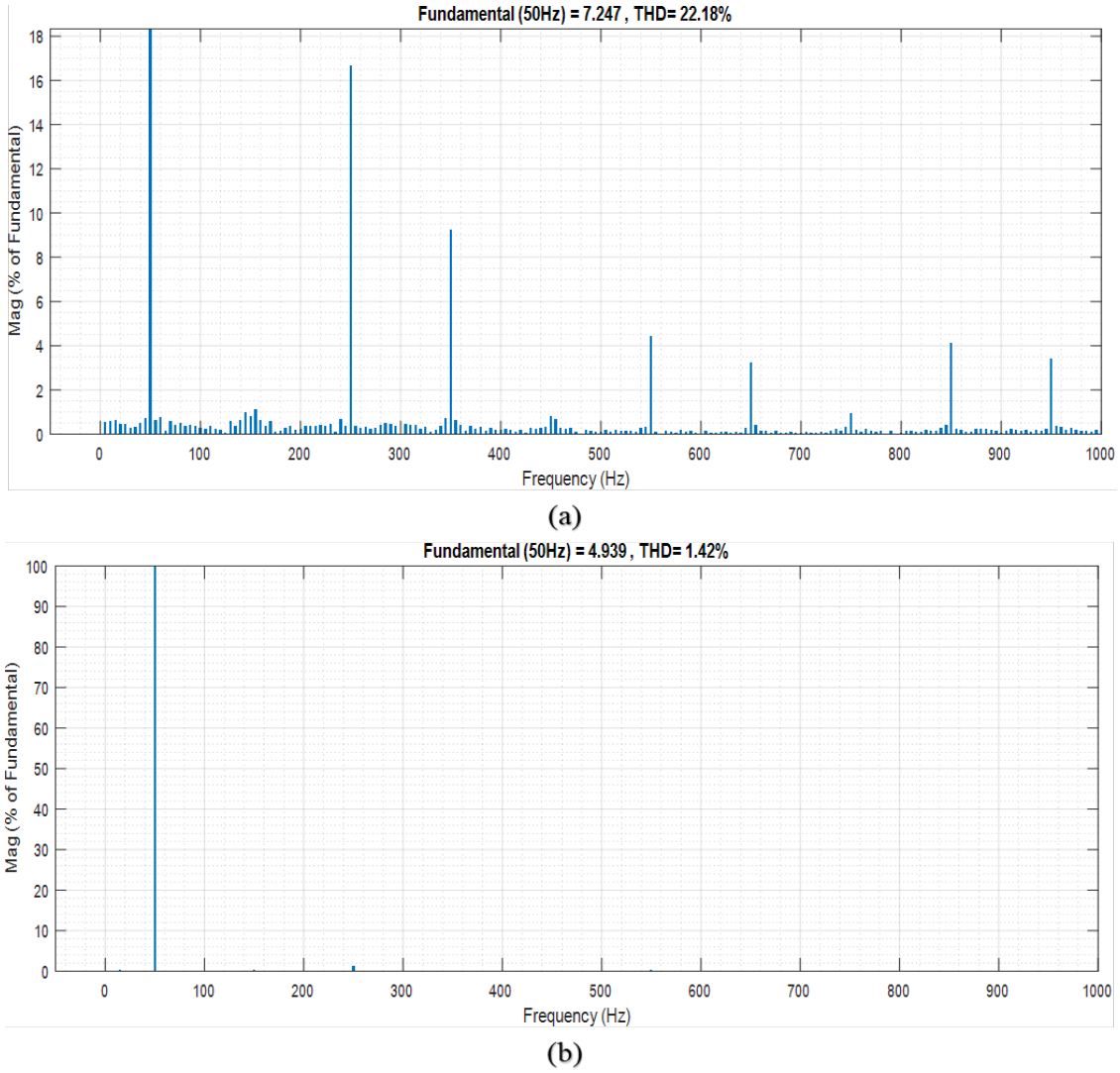

Fig .6. Simulation result of THD value for unbalanced nonlinear load with DSTATCOM (a) load current and (b) grid current.

3.2 Hardware in loop (HIL) simulation result

In the steady-state response simulations, Figure 7 shows an example of a situation where nonlinear loads are present but the DSTATCOM is absent. When the load is connected and the DSTATCOM is introduced, Figure 6(a) shows that the load current's THD value now matches the grid currents. This reduction, as indicated in figure 7(a), comfortably places it within the IEEE-519 standard's acceptable 5% limit. In this instance, the source current waveform only exhibits sinusoidal characteristics and is free of distortions. The net effect is that the Voltage Source Inverter (VSI) effectively supplies the necessary harmonics at the Point of Common Coupling (PCC) to satisfy the demands of the nonlinear load. The grid current exhibits sinusoidal characteristics as a result, and its THD value stays well within the permitted range. This successful conclusion highlights how well the suggested frequency-domain-based VRC control strategy works to mitigate harmonics in the grid system.

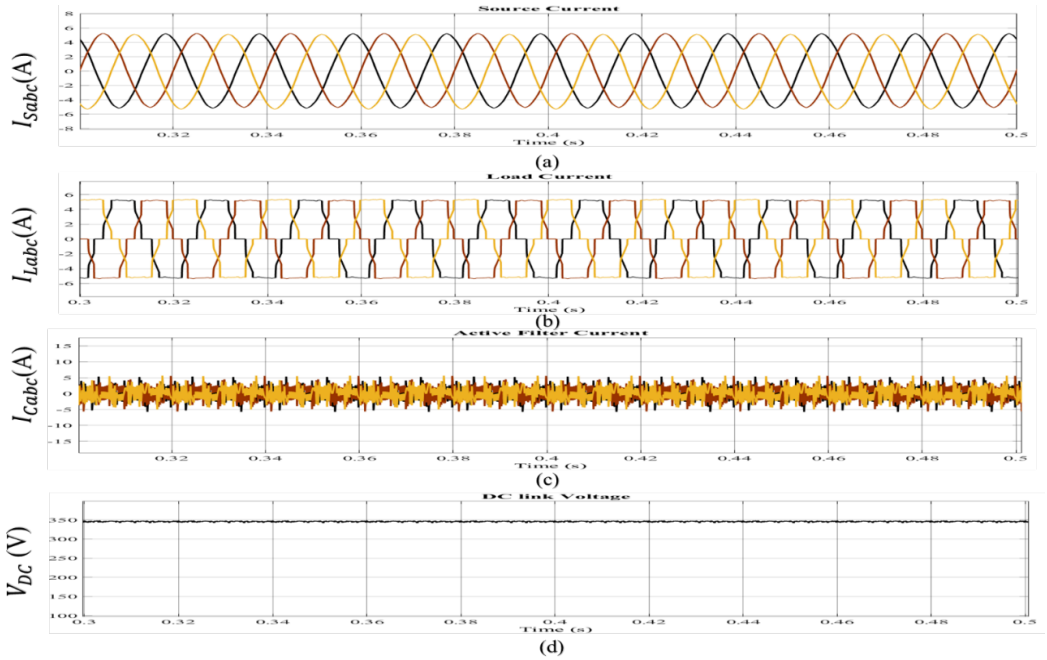

Fig .7. Steady state condition of the DSTATCOM. (a) Source current (I_{sa} ,I_{sb} & I_{sc}) (b) Load current (I_{La} ,I_{Lb} & I_{Lc}) (c) Active Filter current (I_{ca} ,I_{cb} & I_{cc}) and (d) DC link voltage (V_{DC})

Figure 8 displays the results of the FFT spectrum analysis along with the Total Harmonic Distortion (THD) for the source and load currents. Figure 8(a) shows that the THD percentage of the load current is 17.43%. However, Figure 8(b) demonstrates that the THD percentage of the source current is measured at 1.89%, comfortably falling below the 5% limit established by the IEEE 519:2014 standard. This result shows the good cooperation between the frequency-domain based Voltage Reference Configuration (VRC) control method and the proposed DSTATCOM. It significantly lowers the THD of the load current and effectively reduces harmonic distortion, which enhances the quality of the source current.

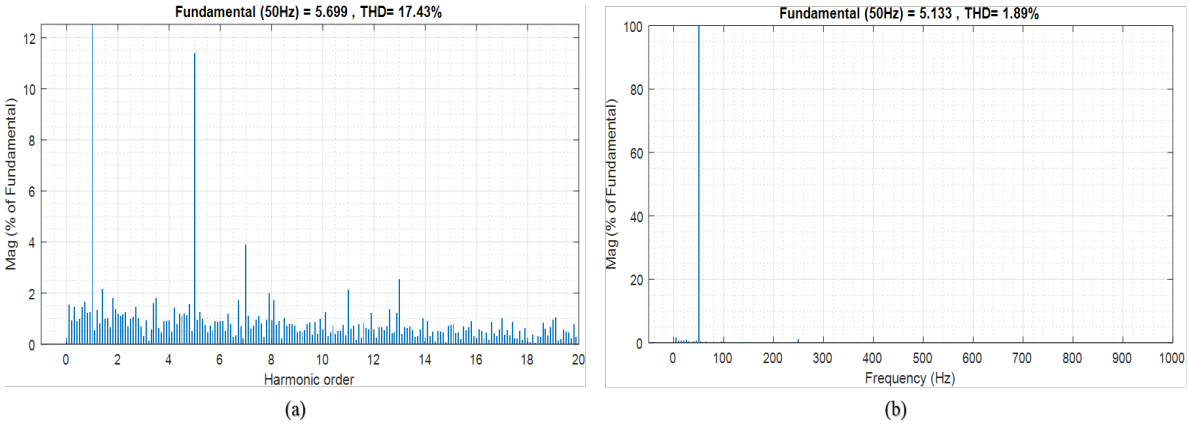

Fig .8. Simulation result of THD value for unbalanced nonlinear load with DSTATCOM (a) load current and (b) grid current.

3.3 Prototype results

The findings of an analysis performed on the DSTATCOM prototype prior to DSTATCOM compensation are displayed in Figure 9. It is evident that the THD for each source current phase exceeded the IEEE-519:2014 standard's allowable limit.

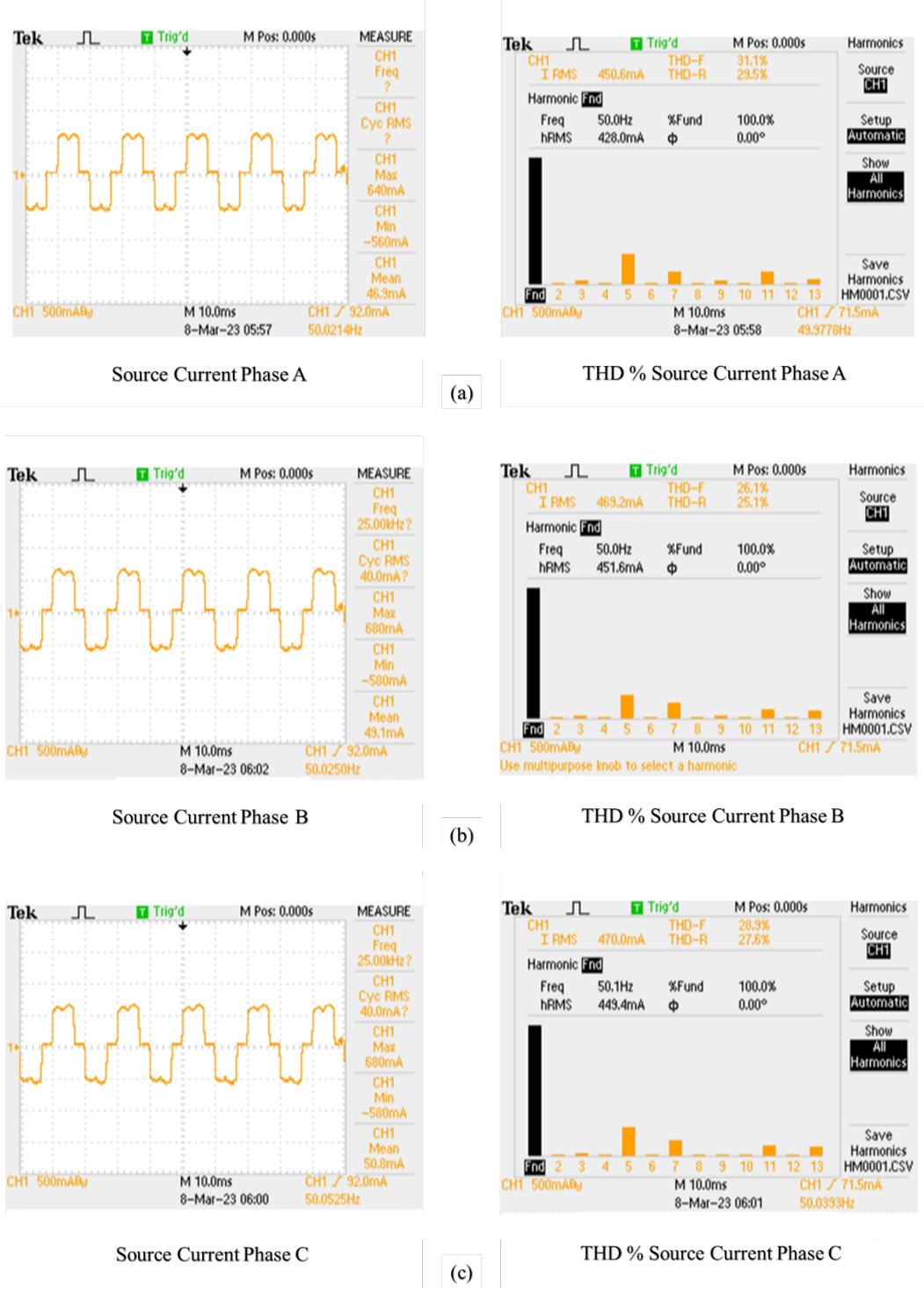

Fig .9. DSTATCOM Prototype under Non-Linear Load Before Compensation (a),(b),(c) Source current (I_{Sa} ,I_{Sb} & I_{Sc}) and THD% of Source current (I_{Sa} ,I_{Sb} & I_{Sc})

The results of the analysis performed on the DSTATCOM prototype after DSTATCOM compensation are shown in Figure 10. As seen in Figures 10(a), (b), and (c), these results show a significant improvement towards near sinusoidal profiles in the source current waveforms for each phase (Isa, Isb, and Isc). In addition, each phase's Total Harmonic Distortion (THD%) has significantly decreased, recording values of 9.64%, 9.78%, and 9.54%, respectively. These numbers show a significant 32% drop from the THD readings before the compensation was put in place. This illustrates how well the frequency domain-based Voltage Reference Configuration (VRC) control algorithm preserves the sinusoidal characteristics of the source currents while compensating for the required harmonics of the load current. Additionally, this nearly meets the requirement outlined by the IEEE-519:2014 standard, which prescribes a maximum THD for line currents at 8% to guarantee secure and efficient power system operation. In conclusion, the THD values in the source currents have been successfully decreased by the integration of the frequency domain-based VRC control algorithm in the DSTATCOM. This demonstrates how well this strategy works to improve power quality and guarantee the power system runs smoothly.

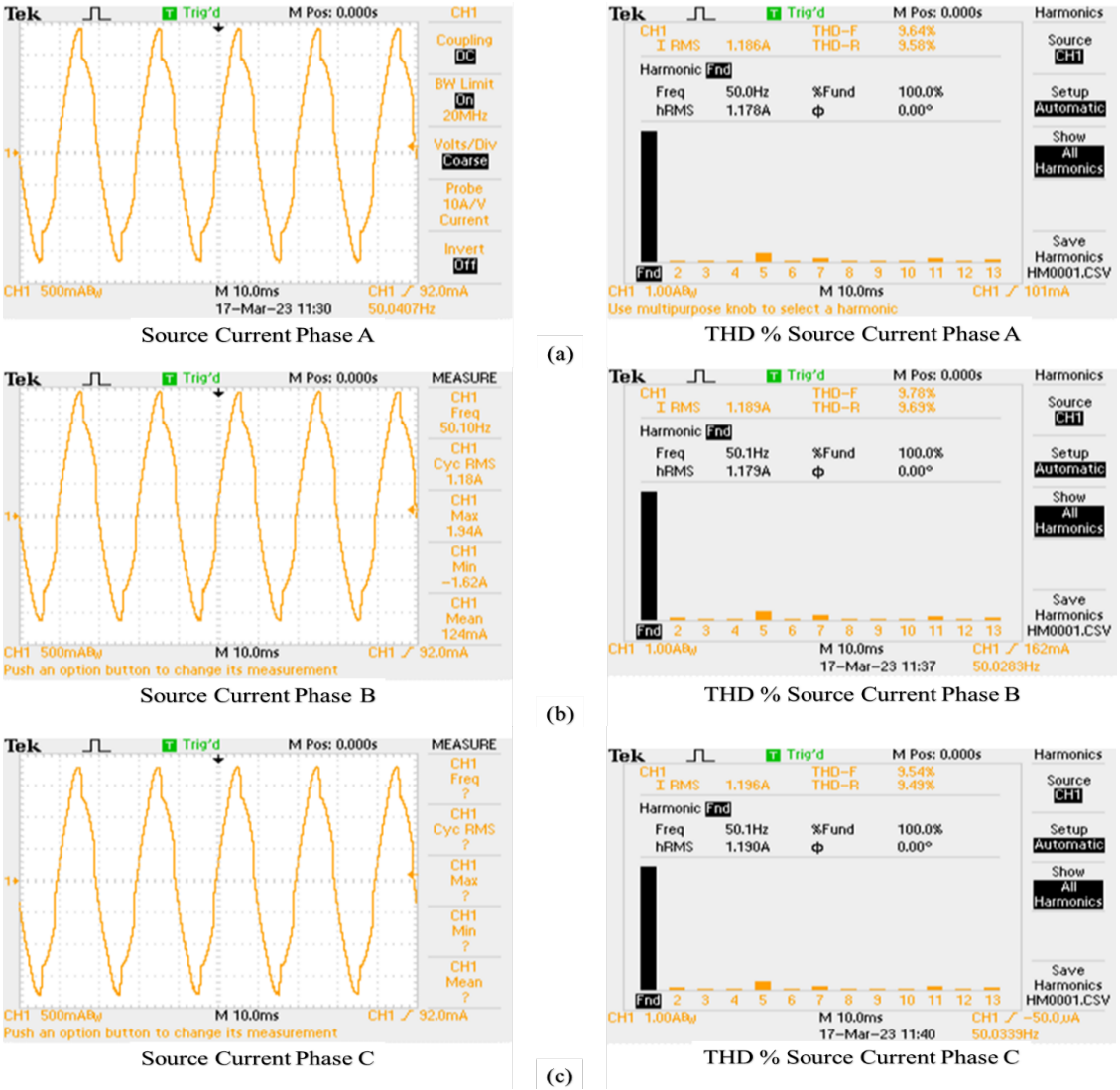

Fig 10. DSTATCOM Prototype under Non-Linear Load After Compensation. (a),(b),(c) Source current (I_{sa} ,I_{sb} & I_{sc}) and THD% of Source current (I_{sa} ,I_{sb} & I_{sc})

4. Conclusions

In summary, this study's goals of improving distribution network power quality by integrating a photovoltaic system and removing harmonics have been successfully met. To address power quality concerns, a reliable approach is to integrate a Distribution Static Synchronous Compensator (DSTATCOM) based on Grid Connected Photovoltaics (PV) into the design and implementation of the system. Additionally, a potent tool for precisely controlling compensating currents has been created: a frequency domain-based Voltage Reference Configuration (VRC) control algorithm created especially for the DSTATCOM based on GCPV. Both simulation-based and hardware validation tests have validated the device's ability to dampen harmonics and reduce Total Harmonic Distortion (THD), demonstrating the potential of the GCPV based DSTATCOM to significantly enhance power quality in distribution systems. This achievement signifies a substantial contribution to-ward enhancing the reliability and efficiency of electrical grids.

Acknowledgement
The author would like to acknowledge the support from the Fundamental Research Grant Scheme (FRGS) under a grant number of FRGS/1/2020/TK0/UNIMAP/02/113 from the Ministry of Education Malaysia.

References

[1] R. Ingale, "Harmonic Analysis Using FFT and STFT," *Int. J. Signal Process. Image Process. Pattern Recognit.*, vol. 7, no. 4, pp. 345–362, 2014, doi: 10.14257/ijsip.2014.7.4.33.
[2] I. Standards, C. Committee, D. Generation, and E. Storage, *IEEE Std 1547.2-2008 IEEE Application Guide for IEEE Std 1547, IEEE Standard for Interconnecting Distributed Resources with Electric Power Systems*, no. April. 2009.
[3] "What Does Power Quality Mean & Why Is It Important - Power Quality Systems International LLC." .
[4] P. Kiss and G. G. Balazs, "Double Domain Simulation - modelling the harmonic effect of different nonlinear loads," in *2014 16th International Conference on Harmonics and Quality of Power (ICHQP)*, May 2014, pp. 395–399, doi: 10.1109/ICHQP.2014.6842873.
[5] M. McGranaghan, "Controlling harmonics from nonlinear loads in commercial facilities," *Proc. Int. Conf. Harmon. Qual. Power, ICHQP*, vol. 2, pp. 872–877, 1998, doi: 10.1109/ICHQP.1998.760157.
[6] M. Irwanto *et al.*, "Photovoltaic powered DC-DC boost converter based on PID controller for battery charging system," *J. Phys. Conf. Ser.*, vol. 1432, no. 1, 2020, doi: 10.1088/1742-6596/1432/1/012055.
[7] A. H. Faranadia, A. M. Omar, and S. Z. M. Noor, "Power Quality Assessment of Grid Connected Photovoltaic System on Power Factor," *2018 110th AEIT Int. Annu. Conf. AEIT 2018*, no. August 2019, 2018, doi: 10.23919/AEIT.2018.8577408.
[8] A. Chandra, B. Singh, B. N. Singh, and K. Al-Haddad, "An improved control algorithm of shunt active filter for voltage regulation, harmonic elimination, power-factor correction, and balancing of nonlinear loads," *IEEE Trans. Power Electron.*, vol. 15, no. 3, pp. 495–507, 2000, doi: 10.1109/63.844510.
[9] O. Gandhi, D. S. Kumar, C. D. Rodríguez-Gallegos, and D. Srinivasan, "Review of power system impacts at high PV penetration Part I: Factors limiting PV penetration," *Sol. Energy*, vol. 210, no. June, pp. 181–201, Nov. 2020, doi: 10.1016/j.solener.2020.06.097.
[10] D. M. Tobnaghi and R. Vafaei, "The impacts of grid-connected photovoltaic system on Distribution networks- A review," *ARPN J. Eng. Appl. Sci.*, vol. 11, no. 5, pp. 3564–3570, 2016.
[11] M. P. Kazmierkowski, *Power Quality: Problems and Mitigation Techniques [Book News]*, vol. 9, no. 2. 2015.
[12] N. Kumar, B. Singh, B. K. Panigrahi, and S. Member, "LLMLF-Based Control Approach and LPO MPPT Technique for Improving Performance of a Multifunction Three-Phase Two-Stage Grid Integrate PV system," *IEEE Trans. Sustain. ENERGY, VOL. 11, NO. 1, JANUARY 2020*, vol. 11, no. 1, pp. 371–380, 2020.
[13] B. Singh and J. Solanki, "A Comparison of Control Algorithms for DSTATCOM," *IEEE Trans. Ind. Electron.*, vol. 56, no. 7, pp. 2738–2745, Jul. 2009, doi: 10.1109/TIE.2009.2021596.
[14] B. Singh, K. Al-Haddad, and A. Chandra, "A new control approach to three-phase active filter for harmonics and reactive power compensation," *IEEE Trans. Power Syst.*, vol. 13, no. 1, pp. 133–138, 1998, doi: 10.1109/59.651624.
[15] N. H. Baharudin, T. M. N. T. Mansur, S. I. S. Hassan, P. Saad, R. Ali, and M. Y. Lada, "A comparison of distribution

static synchronous compensator (dstatcom) control algorithms for harmonic elimination," *ARPN J. Eng. Appl. Sci.*, vol. 10, no. 22, pp. 10740–10744, 2015.

[16] H. Magnago, H. Figueira, O. Gagrica, and D. Majstorovic, "HIL-based certification for converter controllers: Advantages, challenges and outlooks (Invited Paper)," *Proc. 2021 21st Int. Symp. Power Electron. Ee 2021*, 2021, doi: 10.1109/Ee53374.2021.9628196.

[17] "Fast Fourier transform (FFT) of input - Simulink." .

[18] "Implement logic signals as Boolean data (vs. double) - MATLAB & Simulink." .

[19] M. A. Hassan and Y. He, "Constant Power Load Stabilization in DC Microgrid Systems Using Passivity-Based Control with Nonlinear Disturbance Observer," *IEEE Access*, vol. 8, no. May, pp. 92393–92406, 2020, doi: 10.1109/ACCESS.2020.2992780.

[20] A. Banerji, S. K. Biswas, and B. Singh, "DSTATCOM control algorithms: A review," *Int. J. Power Electron. Drive Syst.*, vol. 2, no. 3, pp. 285–296, 2012, doi: 10.11591/ijpeds.v2i3.515.